Cellulose (2021) 28:897–909
https://doi.org/10.1007/s10570-020-03561-4

ORIGINAL RESEARCH

A pH-responsive carboxymethyl cellulose/chitosan hydrogel for adsorption and desorption of anionic and cationic dyes

Wei Wang · Jinjing Hu · Rundong Zhang · Chao Yan · Li Cui · Junjiang Zhu

Received: 17 May 2020 / Accepted: 28 October 2020 / Published online: 23 November 2020
© Springer Nature B.V. 2020

Abstract A carboxymethyl cellulose/chitosan interpenetrating network hydrogel was prepared to adsorb and desorb anionic and cationic dyes applying different pH conditions. The three-dimensional network structure of the hydrogel was investigated using Scanning Electron Microscopy (SEM). Fourier Transform Infrared (FT–IR) was used to analyze the bonding mechanism of the hydrogel. The compression modulus of the hydrogel under neutral conditions exhibited an increase in parallel with the increase of carboxymethyl cellulose content. Under alkaline conditions, the swelling properties of hydrogels in water were enhanced with the increase of the carboxymethyl cellulose content. On the other hand, under acidic conditions, the swelling performance of hydrogels in water was decreased with the increase of carboxymethyl cellulose content. The adsorption capacity and desorption ratio of carboxymethyl cellulose/chitosan hydrogel for Acid Orange II were higher than 100 mg/g and 90%, respectively, while for Methylene Blue were higher than 110 mg/g and 95% even after five adsorption/desorption cycles. This study suggests that the carboxymethyl cellulose/chitosan interpenetrating network hydrogel showed different swelling behaviors under different pH values, which could present great potential as carrier materials in the controllable release-based applications.

W. Wang · J. Hu · R. Zhang · C. Yan (✉) · L. Cui (✉) · J. Zhu
Hubei Key Laboratory of Biomass Fibers and Eco-Dying and Finishing, Wuhan Textile University, Wuhan 430073, Hubei, China
e-mail: yanchao18306@163.com

L. Cui
e-mail: cuili@wtu.edu.cn

Graphic abstract

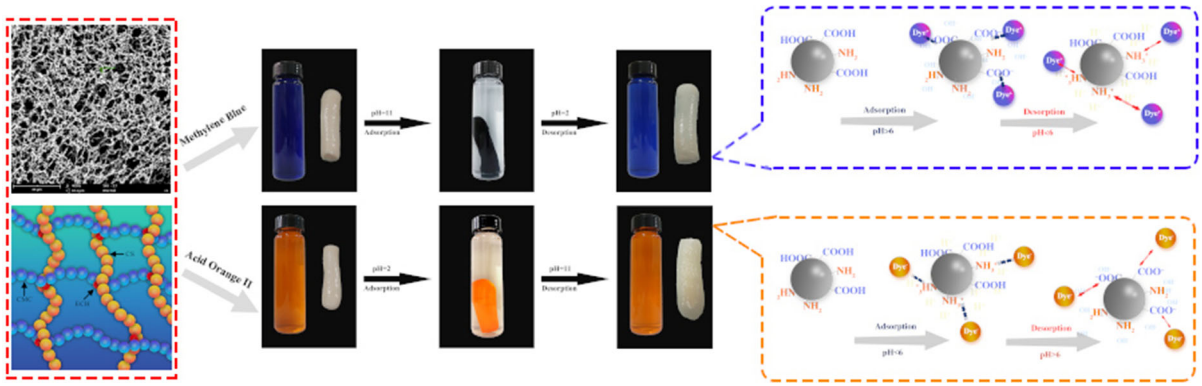

Keywords Interpenetrating network hydrogel · Swelling reversibility · pH response · Adsorption/desorption

Introduction

In the last decades, the textile industry in Asia and especially in China, has developed rapidly and became the world's largest textile producer and exporter (Chang and Ha-Brookshire 2011). Although the textile industry has brought economic prosperity, it has also brought challenges involving pollution. Due to the extensive use of new dyes and auxiliary chemicals, the composition of wastewater containing printing and textile dyes has become more-and-more complex. Therefore, printing and dyeing wastewater has become the primary pollution in the textile industry (Lotito et al. 2012).

The methods of treating printing and dyeing wastewater could mainly include chemical oxidation (Luan et al. 2017), electrochemical (He et al. 2018), and adsorption method (Khamparia and Jaspal 2017), and some new approaches, such as photocatalytic degradation (Li et al. 2019), membrane separation (Li et al. 2018), and/or biological treatment (Xu et al. 2018). Although these methods have shown significant results in wastewater treatment, most of them require harsh process conditions and high costs. As one of the most efficient methods for advanced treatment of printing and dyeing wastewater, adsorption methods usually had low energy consumption and relatively low operational and production costs. Furthermore, they can effectively separate organic pollutants from wastewater without introducing new pollutants (Khamparia and Jaspal 2017). At present, the most used adsorbent materials are the activated carbon-based materials (Li et al. 2013), resin (Pandey et al. 2017), natural minerals (Ngulube et al. 2017) and other solid-phase porous materials with higher costs. These adsorption materials could have issues mainly with unsatisfactory adsorption performance. Therefore, the development of low-cost, highly absorbent and reusable materials has become a research goal. As a natural non-toxic, low-cost and biodegradable raw material, polysaccharides have attracted the interest of researchers.

Cellulose is a high molecular-weight polysaccharide, containing a large number of hydroxyl groups, which has an increased water absorption capacity in nature. However, the hydroxyl group quickly participates in the formation of hydrogen bonds, causing the material to lose its water absorption capacity (Olsson and Salmén 2004). Jia et al. (2016) extracted microcrystalline cellulose from the corn cobs, then prepared carboxymethyl cellulose (CMC) by attaching hydrophilic groups (such as carboxyl groups) through an etherification process, which have enhanced the water absorption of cellulose. Salama (2018) grafted 3-Sulfopropyl methacrylate potassium salt onto CMC in order to prepare hydrogels for the adsorption of cationic dyes, such as Methylene Blue. Toledo et al. (2019) obtained a CMC/poly(acrylic acid) interpenetrating polymer network hydrogel as multifunctional adsorbent.

Chitosan (CS) is the main product of the removal of acetyl groups from natural polyamide chitin. Due to a

large number of hydroxyl and amino groups on its macromolecular chain, chitosan has good adsorption and antibacterial properties (Mohamed and Abd El-Ghany 2012; Naseeruteen et al. 2018; Yang et al. 2018). On the other hand, chitosan is easily soluble in acidic solutions, it has weak water resistance, and mechanical properties (Habiba et al. 2018; Wang and Zhuang 2017), which could limit its applicability in the treatment of printing and dyeing wastewater. Studies have shown that chitosan can be modified by introducing new anionic groups, which could enhance the strength and the acid resistance, by physical or chemical crosslinking, making chitosan to reach significant adsorption and desorption properties (Abu Elella et al. 2019; Karimi et al. 2018).

In this study, CMC and CS were used to prepare an interpenetrating network hydrogel. In water, the carboxylic group on the surface of CMC is ionized to form $-COO^-$. Meanwhile, the amino group located at the surface of CS is protonated to generate NH_3^+ under acidic conditions. Together could form a polyelectrolyte that is insoluble in water due to the electrostatic interaction between the polyionic materials. On the other hand, this situation is not conducive to the formation of the gel. A strong acid was added to the mixed solution to prevent the formation of the electrolyte, and epichlorohydrin was added as a crosslinking agent to prepare the interpenetrating network hydrogel with an amphoteric group. The structural characteristics were investigated by Scanning Electron Microscopy and Fourier Transform Infrared Spectroscopy. Subsequently, the swelling properties of hydrogels were also studied under different composition ratios and pH conditions. The typical adsorption and desorption ability of hydrogels to anionic (Acid Orange II) and cationic (Methylene Blue) dyes were also explored. This paper provides the possibility to broaden the applicability of natural polymer materials such as chitosan and carboxymethyl cellulose in the treatment of printing and dyeing wastewater.

Experimental

Materials

Carboxymethyl cellulose (CMC) ($M_W = 2.4 \times 10^4$ g/mol with a degree of carboxymethyl substitution of 0.75) was purchased from Weifang Lite Composite Material Co., Ltd. Chitosan (CS) ($M_W = 5 \times 10^4$ g/mol, degree of deacetylation = 93%) was supplied by Qingdao Yunzhou Biochemistry Co., Ltd. (Qingdao, China). The average particle size of chitosan powder was 0.9 μm. Epichlorohydrin (ECH) was supplied by Shanghai Sinopharm Chemical Co., Ltd. (Shanghai, China). Hydrochloric acid and acetic acid were purchased from Sinopharm Chemical Reagent Co., Ltd, China. Methylene Blue (industrial grade) and Acid Orange II (industrial grade) were purchased from Tianjin Huamaolong Technology Co., Ltd.

Preparation of CMC/CS interpenetrating network gel

An aqueous solution of CMC with a concentration of 2% was prepared, while an aqueous solution of CS with a concentration of 2% was simultaneously obtained under acidic condition (using acetic acid with a volume fraction of 1%). These solutions were mixed with a mass ratio of 8/2, 7/3, 6/4, 5/5, respectively, and the total volume of the mixed solution was 200 mL. The as-obtained mixtures will be further referred to as CMC_8/CS_2, CMC_7/CS_3, CMC_6/CS_4, CMC_5/CS_5. About 1 mL of 36% concentrated hydrochloric acid was added to 100 mL of a sodium carboxymethyl cellulose aqueous solution. Subsequently, 100 mL of chitosan aqueous solution was introduced while stirring. As the white polyelectrolyte emerged, 8 mL of ECH and 1 mL of hydrochloric acid were added and stirring was continued for 30 min. The as-obtained viscous light yellow solution was dispensed into 35 mL test tubes, sealed and placed in a 65 °C thermostatic water bath for 1 h. When the crosslinking completed, the gel was taken out and rinsed, soaked in deionized water for further use.

Measurement and characterization

Fourier transform infrared (FTIR) study

The FTIR spectra were recorded on a TENSOR-27 type Fourier transform infrared spectrometer (Bruker Instruments, Germany) with a resolution of 2 cm^{-1} in the wavenumber range of 400–4000 cm^{-1}. The samples were prepared for the analysis by grinding the dry

blends with KBr and compressing the mixtures to form sheets.

Scanning electron microscopy (SEM)

The CMC_5/CS_5 samples were freeze-dried by a Freeze dryer LGJ-10D (Si Huan Scientific, Beijing). Samples were sliced and investigated by a Hitachi S-4800 scanning electron microscope (Japan) at an acceleration voltage of 5 kV. The surfaces of the samples were subjected to a 10 nm gold spray treatment.

Effect of pH on the swelling properties of the samples

A sample cut into a size of 1 cm × 1 cm × 1 cm was placed in deionized water for 24 h and weighed. They were immersed in buffer solutions with a pH of 2, 7, 11 at a temperature of 25 °C. Taken them out at regular intervals, the excess water was carefully removed from the surface of the sample with filter paper, weighed (with an analytical balance) and recorded. The swelling ratio SR (%) of the sample was calculated according to Eq. (1):

$$\mathrm{SR}(\%) = (W_t - W_0)/W_0 \times 100\% \quad (1)$$

where W_t (g) was the weight of the sample at time t, and W_0 (g) was the dry weight of the sample.

Compression test

The compressive mechanical properties of the hydrogels were tested in the swelling state at ambient temperature, at pH 7, using a small bench tester (EZ-SX500N, SHIMADZU Co., Ltd. Japan). The compression tests of the cylindrical sample (10 mm height, as the cross-sectional area changed with swelling and were measured and calculated separately) were conducted at a crosshead speed of 3 mm min^{-1}. The elastic modulus of hydrogels was determined from the gradient of the stress–strain curves.

Swelling reversibility test

The sample with known mass was sequentially immersed and soaked for one hour in buffer solutions, with pH values of 2, 7, 11 in sequence as one cycle. Then the sample was conducted into the second test cycle after immersing in a buffer solution with pH = 7 for one hour. Before weighed, the surface of each sample was cleared with filter paper. The swelling ratio SR (%) was calculated according to Eq. (1).

Swelling sensitivity test

The samples were immersed in buffer solutions of pH 2, 4, 7, 9, 11 for 24 h, respectively, and then the samples were taken out. The swelling ratio SR (%) of the samples was calculated once more, according to Eq. (1).

Study on adsorption and desorption behavior of hydrogel

The CMC_5/CS_5 samples were weighed, and a part of them was placed in 100 mL of Methylene Blue solution, with a concentration of 0.5 g/L at 25 °C, and the pH was kept at 11. The other samples were placed in Acid Orange II staining solution at the same temperature, concentration and volume, while the pH was kept at 2. After 24 h of adsorption in the dye solution, the absorbance of the dye solution was measured. The concentration of the dye solution was converted according to the standard curve (Cui et al. 2015), and the adsorption efficiency Q_e (mg/g) was calculated according to Eq. (2). Then the sample was taken out, the remaining dye solution was cleaned from the surface of the samples and it was washed away with deionized water, and the samples were desorbed in deionized water with a pH of 2 and 11 respectively at 25 °C for 24 h. The absorbance of the dye solution was measured, and the concentration of the dye solution after desorption was converted according to the calibration curve. The steps mentioned above were repeated twice to have more accurate data. The desorption amount Q_d (mg/g) was calculated according to Eq. (3).

$$Q_e = (C_0 - C_t) * V/M \quad (2)$$

$$Q_d = C_d * V_d/M \quad (3)$$

where C_0 (mg/L) was the initial concentration of the dye solution, C_t (mg/L) was the concentration of the dye solution at the adsorption time t, C_d (mg/L) was the concentration of desorbed dye solution after 24 h, V (L) was the volume of the dye solution, V_d (L) was the volume of deionized water used for desorption, while M (g) was the dry gel quality.

Results and discussion

Infrared spectrum analysis and crosslinking mechanism

FT–IR spectra of CS, CMC and CMC_5/CS_5 could be observed in Fig. 1. The spectra of CS showed overlapping of multiple absorption peak bands at 3445 cm^{-1}, which was assigned to the hydrogen-bonded O–H tensile vibration peak and the N–H tensile vibration absorption peak. The absorption bands at 1657 cm^{-1}, 1599 cm^{-1} and 1323 cm^{-1} were ascribed to the stretching vibrations of the amide I band (C=O bond), the C–N stretching vibration and the N–H deformation vibration of the amide II band and the amide III band, respectively (Madhusudana Rao et al. 2017). The absorption bands at 1077 cm^{-1} and 1031 cm^{-1} were assigned to the stretching vibration peaks of the secondary and the primary alcoholic hydroxyl group, respectively. FT–IR spectrum of CMC showed a stretching vibration of –OH, located at 3447 cm^{-1}, while asymmetric and symmetric stretching vibration of –COOH groups was featured at 1606 and 1420 cm^{-1}, and symmetric and asymmetric vibration of $–COC^{-}$ was found at 1055 cm^{-1} (Rasoulzadeh and Namazi 2017).

After crosslinking, the hydroxyl peak in the CMC_5/CS_5 interpenetrating network gel was significantly narrowed and shifted to a lower frequency of 3441 cm^{-1}. It was suggested that the hydrogen bonds between CMC and CS were significantly reduced, which also could mean that –OH and $–NH_2$ participated in the reaction. The amide I and II bands of CS were shifted to 1625 cm^{-1}, the amide III band was shifted to 1316 cm^{-1}, and the first and second alcohol hydroxyl peaks were shifted to 1109 cm^{-1}, which further confirmed that $–NH_2$ and –OH were involved in the reaction. The asymmetric and symmetric stretching vibration peaks of CMC carboxyl groups were shifted to 1625 cm^{-1} and 1384 cm^{-1} respectively, resulting from the protonation of $–COO^{-}$ with the HCl.

Furthermore, under acidic conditions, the molecular ring chain of ECH was opened. The chlorine at the top was substituted with the hydroxyl group on the surface of CMC, and the other side reacted with the active amino group and hydroxyl group on the CS, to connect the CMC to CS.

SEM characterization of hydrogel

After freeze-drying, the hydrogel could maintain an excellent three-dimensional structure, which was necessary to investigate its three-dimensional network and porous structure using an electron microscope. It could be seen from Fig. 2a that the CMC_5/CS_5 gel presented a dense network and a three-dimensional porous structure and its hole diameter were within the range of 10 μm. This aspect further proved that CMC and CS were crosslinked together under the action of ECH to form the composite hydrogel with a three-dimensional porous structure.

Swelling balance

As shown in Fig. 3a, the swelling ratio of CMC/CS hydrogels increased with the increase of the CS content, wherein the swelling ratio of CMC_5/CS_5 and CMC_6/CS_4 hydrogels reached a yield of 70 g/g when the pH value was 2. The pKa ($–COO^{-}$) value of carboxyl group on the CMC is near 4.8 and the amino pKa ($–NH_3^{+}$) value on the CS is near 6.5 (Yang et al. 2019; Zargar et al. 2015). The swelling of the gel was attributed to the protonated amines at low pH (where CMC was non-charged), so the swelling ratio was the highest at the highest content of CS. The repulsion between charges led to the relaxation of the macromolecular chain. Meanwhile, the affinity of $–NH_3^{+}$ to water molecules also played a significant role, which was favorable to adsorption of larger amounts of water.

At pH = 7 (see Fig. 3b), the four hydrogels with different mass ratio showed a lower swelling ratio in comparison with, between 20 and 30 g/g. Due to the dissociation of CMC (here CS was non-charged), comparing to pH = 2, the swelling ratio at pH = 7 showed a reverse order between four samples. Under neutral conditions, most of the –COOH existed in the form of $–COO^{-}$, and the strong electrostatic repulsion between $–COO^{-}$ increased the hydrogel's ability to absorb water. The hydrogels with more CMC content exhibited increasingly anionic characteristics. Besides, parts of the –COOH, $–NH_2$ and –OH groups formed hydrogen bonds to lead the polymer chain to shrink, resulting in the increased overall swelling capacity.

At pH = 11 (see Fig. 3c), the swelling performance of the hydrogels was pretty good and increased with

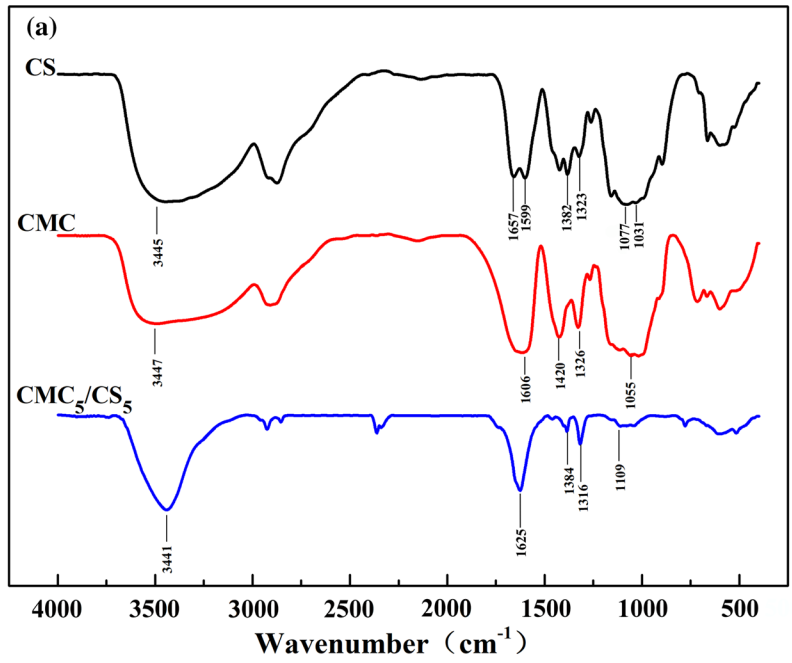

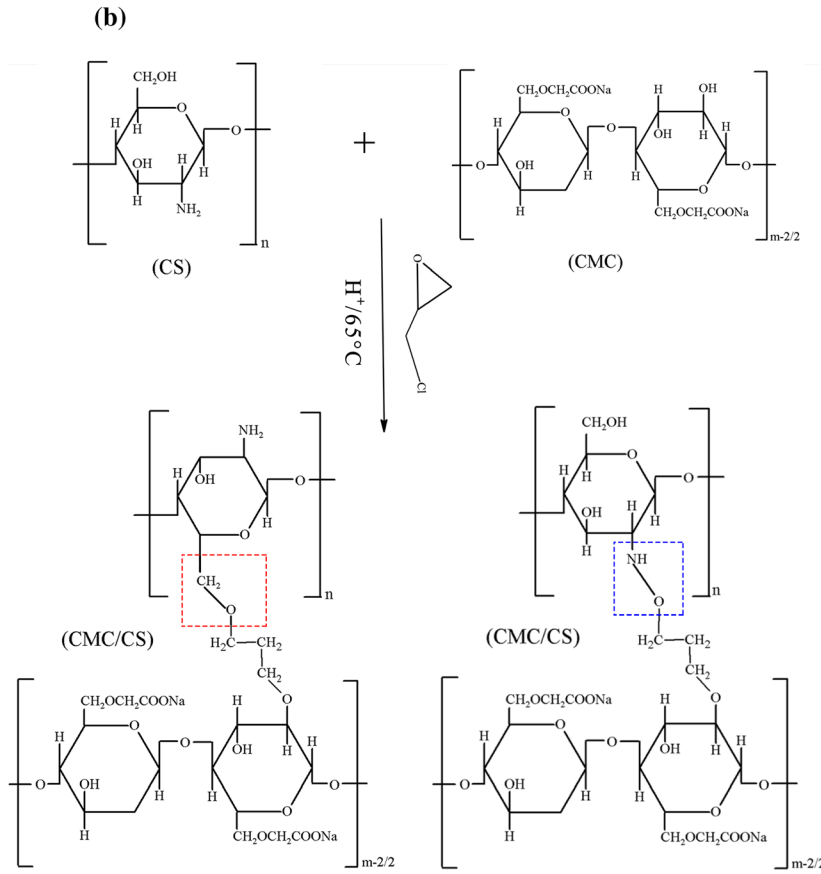

Fig. 1 Infrared spectra of CS, CMC and CMC_5/CS_5 (**a**); proposed reaction mechanism of ECH with CMC and CS (**b**)

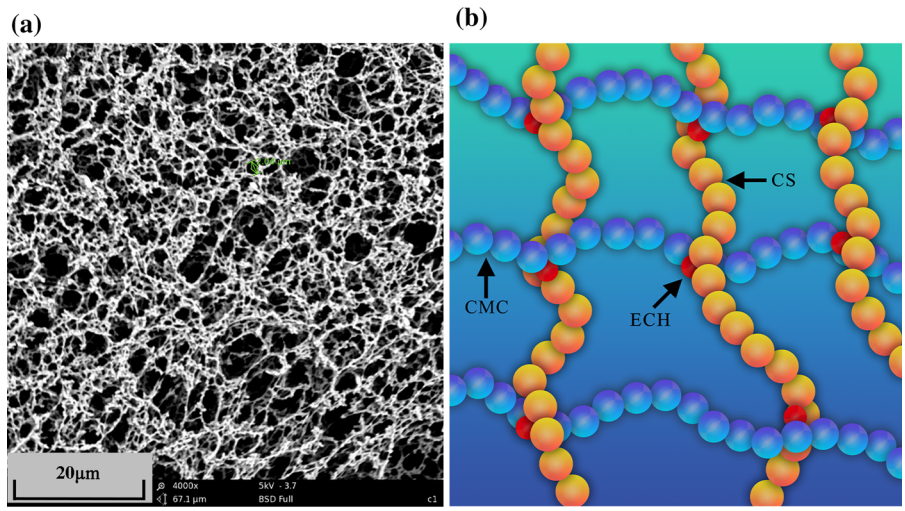

Fig. 2 SEM of CMC_5/CS_5 (**a**) and diagram of CMC/CS cross-linking (**b**)

the increasing content of CMC. The amino groups on CS almost existed in the form of $–NH_2$ under the strong alkaline conditions, where the protonation effect could be neglected. All of the –COOH groups were ionized to $–COO^-$, and the repulsion between molecular chains continued to increase with the increase of CMC content in hydrogels. The molecular chain was significantly stretched, and the water absorption performance was considerably enhanced. Because CMC had higher linear charge density than chitosan, the maximum swelling of the anionically charged hydrogel was the highest at all mixing ratios considering the amount of CMC and chitosan.

Investigations of mechanical performance

The compression stress–strain curves of hydrogels are shown in Fig. 4. When the strain was 80%, the compression stress was 7.9 kPa in the case of CMC_5/CS_5, whereas, in the case of CMC_8/CS_2 was 22.7 kPa. It was also observed that the compression elastic modulus of hydrogels increased in parallel with the increase of the CMC content, and all the hydrogel samples showed analogous curves. It is worth to be noted that the mechanical properties of the hydrogel did not increase following the increase in the degree of crosslinking. Presumably, in the process of compression test, for low-elastic hydrogels with high water content, the pressure could cause the hydrogel to lose water and increase its elastic modulus. It could also be observed in Fig. 3, that the swelling ratio was enhanced with the increase of CMC content at pH = 7. At the same time, as CMC was dissociated a large number of $–COO^-$ at pH 7, the dynamic ionic bonds could also serve as sacrificial bonds to dissipate the energy of the hydrogel network, thus improving the mechanical properties of the absorbent. (Li et al. 2020).

Swelling reversibility

It could be observed from Fig. 5 that after being transferred from pH 2 to pH 7 for one hour, the swelling rates of the hydrogels were all reduced by about half. After being placed at a pH of 11 for one hour, the hydrogels start to swell again, while being immersed in an environment with a pH of 7 (for one hour), the swelling rate began to decrease again. The CMC_5/CS_5 hydrogel showed the highest swelling rate when it was further transferred from pH 7 to pH 2, but its swelling rate was the lowest when it was transferred from pH 7 to pH 11. The hydrogel CMC_8/CS_2 had the highest swelling rate when it was transferred from pH 7 to pH 11, and the swelling rate was significantly increased within 1 h, which caused the decline in the two hours after being transferred to pH 7 and pH 2. After three cycles of testing, it was found that the swelling rate of the hydrogel changed with pH, showing a strong sensitivity and reversibility. The speed and size of the swelling rate change depended mainly on the ratio of CMC and CS in the gel and the pH value of the environment.

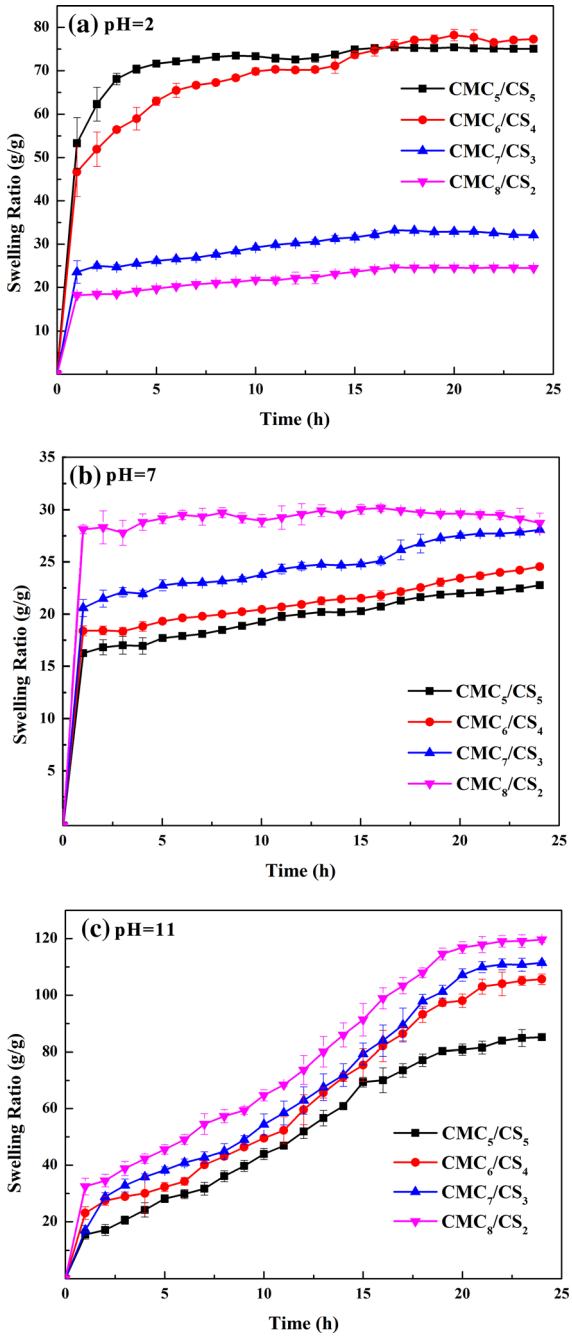

Fig. 3 Swelling performance of CMC/CS hydrogels with different mass ratios at pH 2, 7 and 11, within 24 h

Swelling sensitivity

It could be observed from Fig. 6 that when the pH was between 2 and 4, the swelling rate of CMC_8/CS_2 increased slightly with the increase of the pH, while the other three samples decreased drastically with the increase of pH value. At pH = 4, parts of –COOH existed in the form of $–COO^-$ and generated an internal salt with $–NH_3^+$. Moreover, –COOH and $–NH_2$ were ionic bonded. These factors made the hydrogel network tightly bonded so that water was not easy to access the swelling volume. The excess of CMC carboxyl groups in CMC_8/CS_2 was partially ionized to $–COO^-$ and was combined all of $–NH_3^+$. The other part of $–COO^-$ generated an electrostatic repulsion, which weakened the network structure and caused a slight increase of the swelling rate.

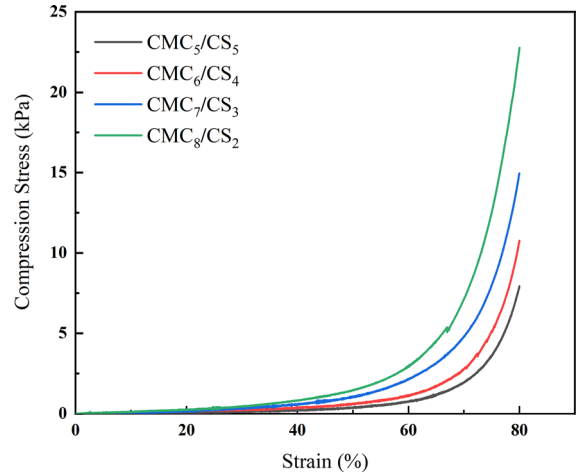

Fig. 4 Compression stress–strain curves of hydrogels

As shown in Fig. 6, when the pH value was between 4 and 9, the swelling ratio of all the samples increased slightly with the increase of pH. As the degree of ionization of –COOH groups increased, the number of $–COO^-$ ions also increased. While a large amount of deprotonated $–NH_3^+$ was formed, the bonds connected with $–COO^-$ ion became less. The increase of the electrostatic repulsion force led to the stretch of the macromolecular chain.

At pH = 4, the swelling ratio was the lowest. This ratio could be attributed to the charge balance between partially dissociated –COOH groups, partially protonated $–NH_2$ groups and the formation of polyelectrolyte complex inside the hydrogel. When the pH value was between 9 and 11, $–COO^-$ was the dominant state of –COOH, and $–NH_3^+$ was completely deprotonated, so the electrostatic repulsion was significantly enhanced and played a leading role. The swelling ratios of the hydrogels with different ratio increased significantly with increasing pH.

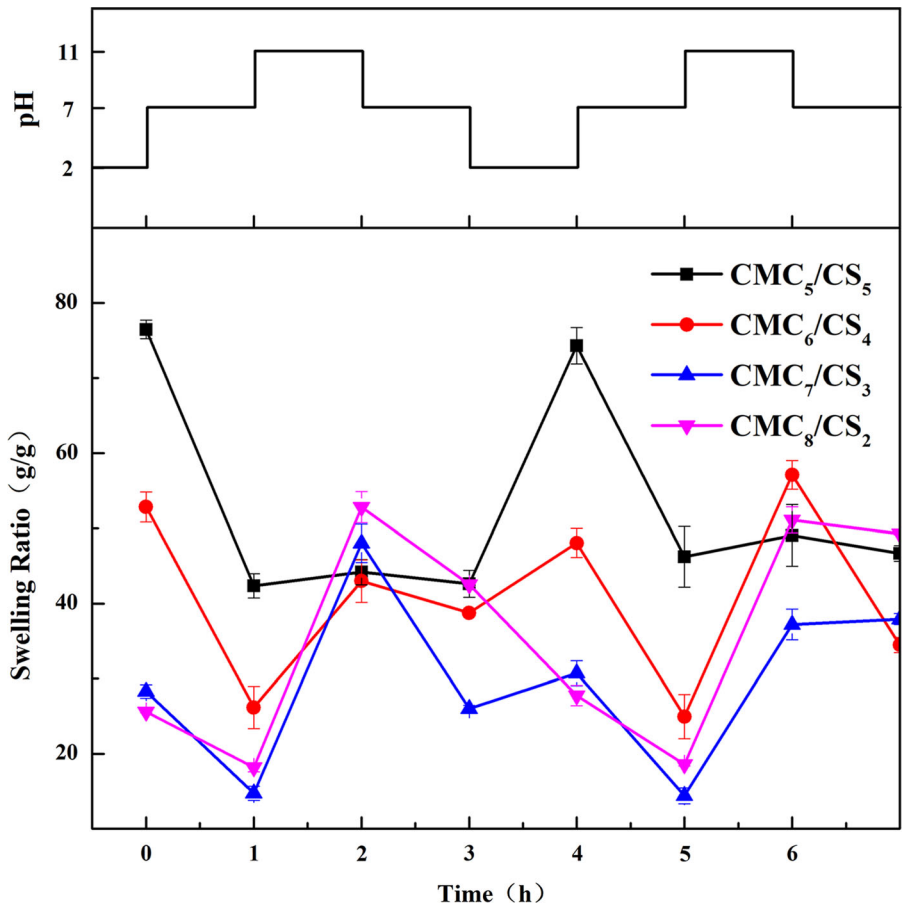

Fig. 5 Cyclic swelling behavior of CMC/CS hydrogels with different mass ratios

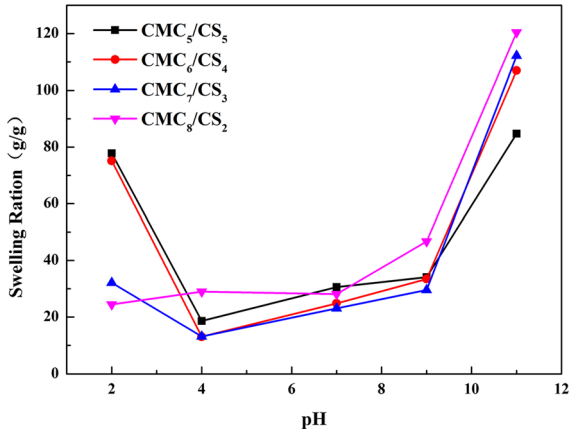

Fig. 6 Swelling properties of CMC/CS with different mass ratios at different pH

It could be already known from the equilibrium theory that during the swelling process, water was swelled mainly by the osmotic pressure, generated by the difference in free ion concentration between inside and outside of the gel (Yu et al. 2014). The acidic and alkaline environment could protonate the amino groups or ionize the carboxyl groups in the gel, which could make the free ion concentration inside the gel higher than that in the environment. The resulting osmotic pressure could cause the interpenetrating network gel to absorb water and swell.

Adsorption and desorption

It could be observed from Fig. 7 that the adsorption capacity of the CMC_5/CS_5 hydrogel toward Methylene Blue dye could reach more than 120 mg/g and the desorption rate could reach 95% within five cycles. The Q_e of Acid Orange II dye could reach more than 100 mg/g, while the desorption rate could reach 90% within five cycles. In the first three cycles, the Q_e of

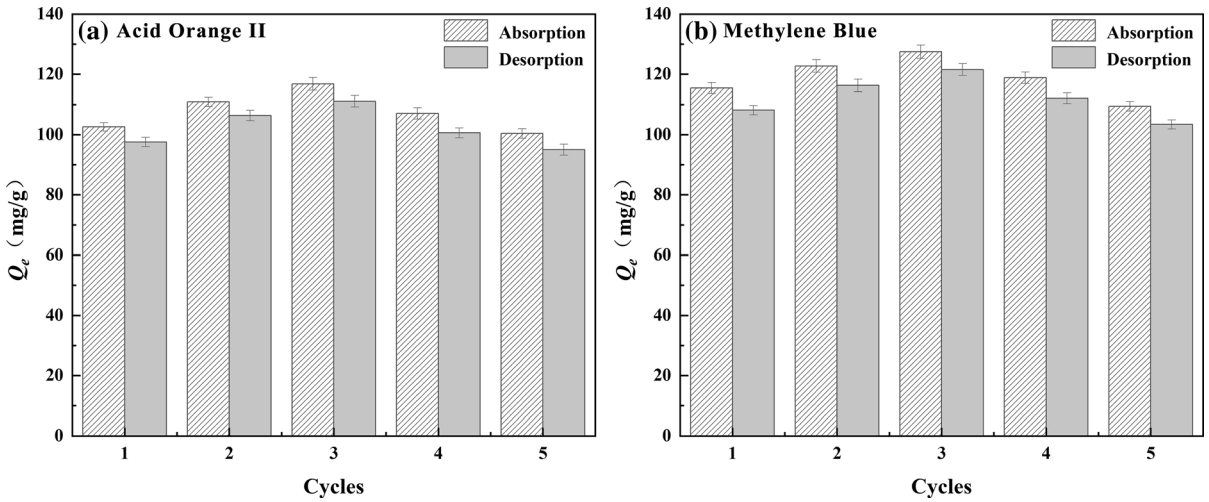

Fig. 7 Five cycles of adsorption and desorption of Acid Orange II and Methylene Blue by CMC_5/CS_5 hydrogel

Methylene Blue increased with the increase of the number of cycles. The swelling performance was improved after desorption under acidic conditions (see Fig. 3), resulting in higher absorption of Methylene Blue under alkaline conditions.

Similarly, the Q_e of Acid Orange II in the third cycle was also higher than that observed in the first and second cycles. Thus, the CMC_5/CS_5 hydrogel desorbed under alkaline conditions, and its swelling performance was be improved in comparison with the

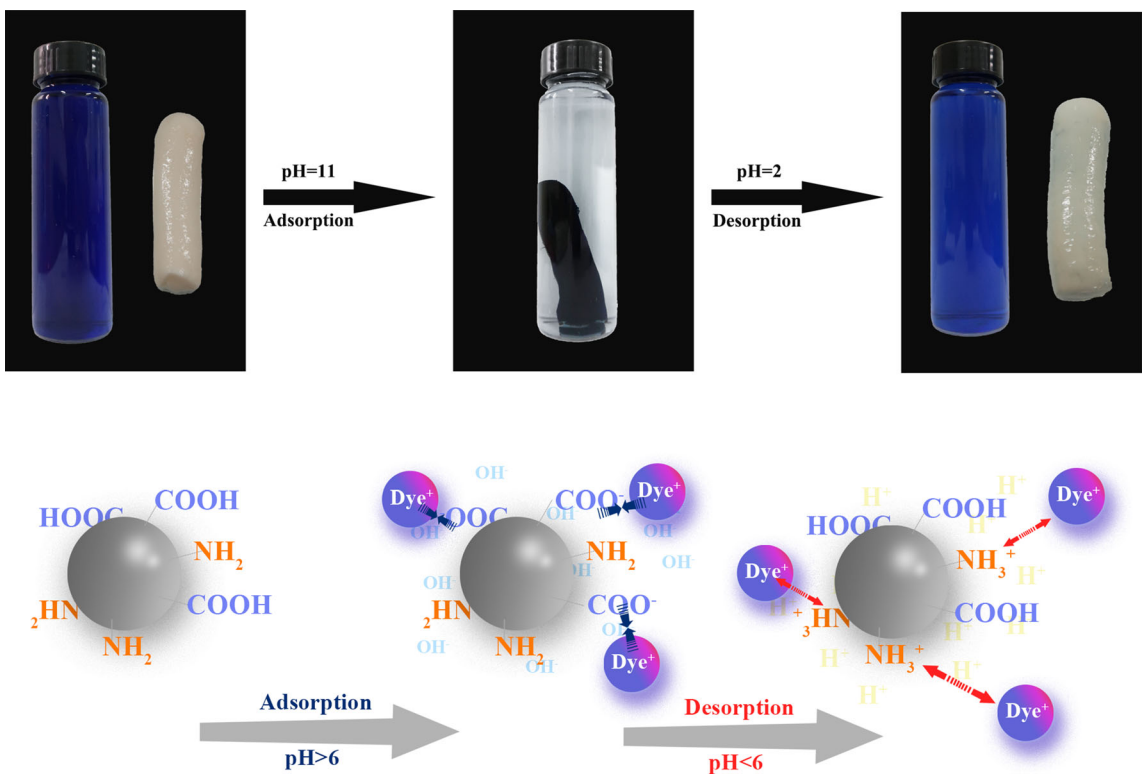

Fig. 8 Schematic diagram and working mechanism of CMC_5/CS_5 adsorption and desorption of Methylene Blue

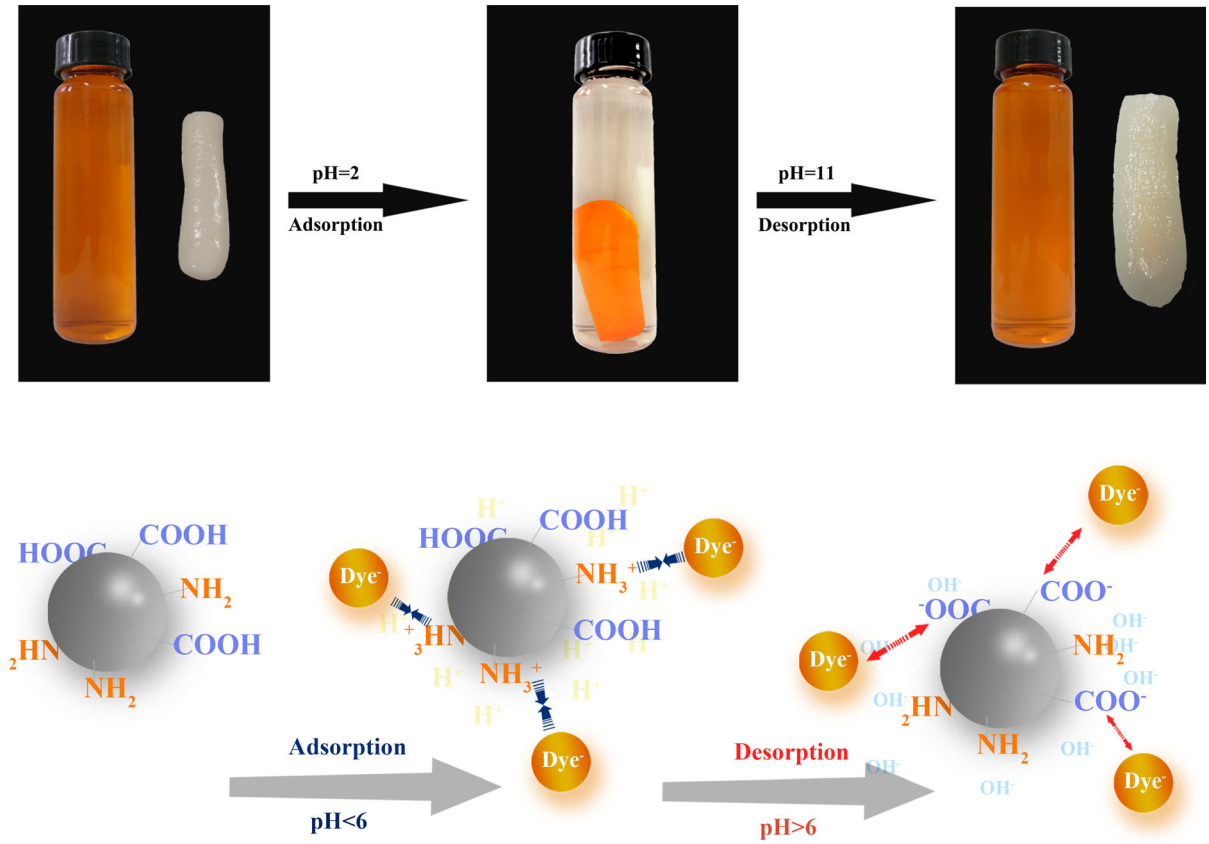

Fig. 9 Schematic diagram and working mechanism of CMC_5/CS_5 adsorption and desorption of Acid Orange II

neutral environment (see Fig. 3), and Acid Orange II dyes could be adsorbed under acidic conditions with higher efficiency. However, in the fourth and fifth cycles, the Q_e decreased. This behavior might be attributed to the fact that after the first three cycles, the swelling reversibility of the hydrogel was reduced, while, undesorbed dye occupied ionic bond sites, which led to a decrease in the total adsorption capacity.

As shown in Figs. 8 and 9, under alkaline conditions, the carboxyl groups on the CMC_5/CS_5 hydrogel existed in their ionized form ($–COO^-$), which could be employed to bind the positively charged Methylene Blue by electrostatic interaction, thereby achieving enhanced adsorption efficiency. Under acidic conditions, carboxyl groups on the hydrogel were kept in the form of –COOH which was not favorable to adsorb the positively charged Methylene Blue. Moreover, the protonated amino groups ($–NH_3^+$) removed Methylene Blue from the hydrogel through electrostatic repulsion to achieve the purpose of desorption. Under the acidic condition, the protonated amino groups ($–NH_3^+$) on the surface of CMC_5/CS_5 hydrogel could adsorb the negatively charged Acid Orange II by electrostatic interaction. Under alkaline conditions, amino groups on the hydrogel were kept in the form of $–NH_2$ which was not available to adsorb the negative Acid Orange II. Furthermore, the ionized carboxyl group ($–COO^-$) allowed to remove the Acid Orange II dye from the hydrogel through electrostatic repulsion to achieve the purpose of desorption (Cui et al. 2015).

Conclusions

In the present work, the interpenetrating network hydrogel was prepared by crosslinking CMC and CS with epichlorohydrin. Under acidic conditions, the hydrogels presented good pH sensitivity, swelling reversibility, adsorption and desorption properties

toward Methylene Blue and Acid Orange II dye. Different mass ratios of CMC and CS hydrogels have shown different swelling responses toward pH. CS mainly dominated the swelling performance under acidic conditions and CMC under alkaline conditions. The swell capability of CMC_5/CS_5 hydrogel reached above 70 g/g at pH 2, and that of CMC_8/CS_2 hydrogel reached 110 g/g at pH 11. CMC_5/CS_5 hydrogels adsorbed 100 mg/g Acid Orange II dyes at pH 2 within five cycles and had a desorption rate higher than 90%. At pH 11, the adsorbed amount of Methylene Blue dyes was 120 mg/g, and the desorption rate reaching 95%. The significant swelling property of carboxymethyl cellulose/chitosan interpenetrating network hydrogel could provide the possibility to be applied in the dye adsorption of specific sites and controlled drug release.

Acknowledgments The authors gratefully acknowledge to Analysis and Testing Center of Wuhan Textile University for testing service and the Central Committee Guides Local Science and Technology Development Special Project of Hubei Province (2019ZYYD073) for financial support.

Compliance with ethical standards

Conflict of interest The authors declare that they have no conflicts of interest.

References

Abu Elella MH, ElHafeez EA, Goda ES, Lee S, Yoon KR (2019) Smart bactericidal filter containing biodegradable polymers for crystal violet dye adsorption. Cellulose 26:9179–9206. https://doi.org/10.1007/s10570-019-02698-1

Chang T-T, Ha-Brookshire J (2011) Business activities, competitive resources and ownership types of Chinese textile and apparel manufacturing firms. Int J Fash Des Technol Edu 4:115–125. https://doi.org/10.1080/17543266.2011.560578

Cui L, Xiong Z, Guo Y, Liu Y, Zhao J, Zhang C, Zhu P (2015) Fabrication of interpenetrating polymer network chitosan/gelatin porous materials and study on dye adsorption properties. CarbohydrPolym 132:330–337. https://doi.org/10.1016/j.carbpol.2015.06.017

Habiba U, Siddique TA, Li Lee JJ, Joo TC, Ang BC, Afifi AM (2018) Adsorption study of methyl orange by chitosan/polyvinyl alcohol/zeolite electrospun composite nanofibrous membrane. CarbohydrPolym 191:79–85. https://doi.org/10.1016/j.carbpol.2018.02.081

He W, Liu Y, Ye J, Wang G (2018) Electrochemical degradation of azo dye methyl orange by anodic oxidation on Ti_4O_7 electrodes. J Mater Sci Mater Electron 29:14065–14072. https://doi.org/10.1007/s10854-018-9538-6

Jia F, Liu H-J, Zhang G-G (2016) Preparation of carboxymethyl cellulose from corncob. Proced Environ Sci 31:98–102. https://doi.org/10.1016/j.proenv.2016.02.013

Karimi AR, Rostaminezhad B, Khodadadi A (2018) Effective removal of a cobalt-tetrasulfonatedphthalocyanine dye from an aqueous solution with a novel modified chitosan-based superabsorbent hydrogel. J ApplPolymSci 135:46167. https://doi.org/10.1002/app.46167

Khamparia S, Jaspal DK (2017) Adsorption in combination with ozonation for the treatment of textile waste water: a critical review. Front Environ SciEng 11:8. https://doi.org/10.1007/s11783-017-0899-5

Li Y et al (2013) Comparative study of methylene blue dye adsorption onto activated carbon, graphene oxide, and carbon nanotubes. ChemEng Res Des 91:361–368. https://doi.org/10.1016/j.cherd.2012.07.007

Li F, Huang J, Xia Q, Lou M, Yang B, Tian Q, Liu Y (2018) Direct contact membrane distillation for the treatment of industrial dyeing wastewater and characteristic pollutants. Sep PurifTechnol 195:83–91. https://doi.org/10.1016/j.seppur.2017.11.058

Li Y et al (2019) Enhanced photocatalytic degradation of organic dyes via defect-rich TiO_2 prepared by dielectric barrier discharge plasma. Nanomaterials. https://doi.org/10.3390/nano9050720

Li N, Hu Y-J, Bian J, Li M-F, Hao X, Peng F, Sun R-C (2020) Enhanced mechanical performance of xylan-based composite hydrogel via chain extension and semi-interpenetrating networks. Cellulose 27:4407–4416. https://doi.org/10.1007/s10570-020-03080-2

Lotito AM, Fratino U, Bergna G, Di Iaconi C (2012) Integrated biological and ozone treatment of printing textile wastewater. ChemEng J 195:261–269. https://doi.org/10.1016/j.cej.2012.05.006

Luan M, Jing G, Piao Y, Liu D, Jin L (2017) Treatment of refractory organic pollutants in industrial wastewater by wet air oxidation. Arabian J Chem 10:S769–S776. https://doi.org/10.1016/j.arabjc.2012.12.003

Madhusudana Rao K, Kumar A, Han SS (2017) Polysaccharide based bionanocomposite hydrogels reinforced with cellulose nanocrystals: drug release and biocompatibility analyses. Int J BiolMacromol 101:165–171. https://doi.org/10.1016/j.ijbiomac.2017.03.080

Mohamed NA, Abd El-Ghany NA (2012) Synthesis and antimicrobial activity of some novel terephthaloylthiourea cross-linked carboxymethyl chitosan hydrogels. Cellulose 19:1879–1891. https://doi.org/10.1007/s10570-012-9789-y

Naseeruteen F, Hamid NSA, Suah FBM, Ngah WSW, Mehamod FS (2018) Adsorption of malachite green from aqueous solution by using novel chitosan ionic liquid beads. Int J BiolMacromol 107:1270–1277. https://doi.org/10.1016/j.ijbiomac.2017.09.111

Ngulube T, Gumbo JR, Masindi V, Maity A (2017) An update on synthetic dyes adsorption onto clay based minerals: a state-of-art review. J Environ Manag 191:35–57. https://doi.org/10.1016/j.jenvman.2016.12.031

Olsson A-M, Salmén L (2004) The association of water to cellulose and hemicellulose in paper examined by FTIR

spectroscopy. Carbohydr Res 339:813–818. https://doi.org/10.1016/j.carres.2004.01.005

Pandey N, Shukla SK, Singh NB (2017) Water purification by polymer nanocomposites: an overview. Nanocomposites 3:47–66. https://doi.org/10.1080/20550324.2017.1329983

Rasoulzadeh M, Namazi H (2017) Carboxymethyl cellulose/graphene oxide bio-nanocomposite hydrogel beads as anticancer drug carrier agent. CarbohydrPolym 168:320–326. https://doi.org/10.1016/j.carbpol.2017.03.014

Salama A (2018) Preparation of CMC-g-P(SPMA) super adsorbent hydrogels: exploring their capacity for MB removal from waste water. Int J BiolMacromol 106:940–946. https://doi.org/10.1016/j.ijbiomac.2017.08.097

Toledo PVO, Limeira DPC, Siqueira NC, Petri DFS (2019) Carboxymethyl cellulose/poly(acrylic acid) interpenetrating polymer network hydrogels as multifunctional adsorbents. Cellulose 26:597–615. https://doi.org/10.1007/s10570-018-02232-9

Wang J, Zhuang S (2017) Removal of various pollutants from water and wastewater by modified chitosan adsorbents. Crit Rev Environ SciTechnol 47:2331–2386. https://doi.org/10.1080/10643389.2017.1421845

Xu H et al (2018) Recent advances in anaerobic biological processes for textile printing and dyeing wastewater treatment: a mini-review. World J MicrobiolBiotechnol 34:165. https://doi.org/10.1007/s11274-018-2548-y

Yang K, Han Q, Chen B, Zheng Y, Zhang K, Li Q, Wang J (2018) Antimicrobial hydrogels: promising materials for medical application. Int J Nanomed 13:2217–2263. https://doi.org/10.2147/IJN.S154748

Yang J, Dahlström C, Edlund H, Lindman B, Norgren M (2019) pH-responsive cellulose–chitosan nanocomposite films with slow release of chitosan. Cellulose 26:3763–3776. https://doi.org/10.1007/s10570-019-02357-5

Yu J, Yang G, Li Y, Yang W, Gao J, Lu Q (2014) Synthesis, characterization, and swelling behaviors of acrylic acid/carboxymethyl cellulose superabsorbent hydrogel by glow-discharge electrolysis plasma. PolymEngSci 54:2310–2320. https://doi.org/10.1002/pen.23791

Zargar V, Asghari M, Dashti A (2015) A review on chitin and chitosan polymers: structure, chemistry, solubility, derivatives, and applications. ChemBioEng Rev 2:204–226. https://doi.org/10.1002/cben.201400025

Publisher's Note Springer Nature remains neutral with regard to jurisdictional claims in published maps and institutional affiliations.